

## Molecular Environment Effects on Two-Photon-Absorbing Heterocyclic Chromophores

Jeffery W. Baur,\* Max D. Alexander Jr., Michael Banach, Lisa R. Denny, Bruce A. Reinhardt,<sup>†</sup> and Richard A. Vaia\*

Polymer Branch AFRL/MLBP, U.S. Air Force Research Laboratory,  
Wright-Patterson AFB, Ohio 45433

Paul A. Fleitz

Laser Hardening Branch AFRL/MLPJ, U.S. Air Force Research Laboratory,  
Wright-Patterson AFB, Ohio 45433

Sean M. Kirkpatrick

Science Applications International Corporation, Dayton Ohio 45431

Received April 30, 1999. Revised Manuscript Received August 3, 1999

Over the past several years, organic molecules exhibiting significant two-photon absorbance and subsequent up-converted fluorescence have been of intense interest for a wide variety of applications including data storage, imaging, and optical limiting. However, the establishment of structure–property relationships for some asymmetric molecules has been hindered by the sensitivity of these nonlinear optical properties to the local molecular environment and to the pulse width of the incident radiation. To understand the influence of the local molecular environment on the excited states of these two-photon-absorbing molecules, the linear absorbance, the single-photon-excited photoluminescence, and the two-photon-excited photoluminescence of a series of heterocyclic dyes are examined. The stabilization of the longest-lived one-photon-excited state by the local molecular environment can be described by mean field interactions with solvent molecules as given by the Lippert equation. Because the same stabilization dominates the two-photon-induced longest-lived excited state, the influence of the local molecular environment on the two-photon luminescence can be predicted using the Lippert equation and one-photon experiments. These results support models that suggest excited-state absorption is the primary cause of sensitivity of the “effective” two-photon cross-section to the pulse-width and the local molecular environment.

### Introduction

Although the two-photon absorption process was first theoretically predicted in 1931<sup>1</sup> and experimentally confirmed in the 1960s,<sup>2</sup> it was generally considered too weak to be of practical use. However, recently there has been a renewed interest in this area due to the synthesis of organic molecules with substantially increased effective two-photon absorption cross-sections.<sup>3,4</sup> The continued achievement of large nonlinear responses will unleash drastic improvements in capability and performance for a variety of applications including optical limiting,<sup>3,5</sup> nondestructive imaging,<sup>6</sup> data storage,<sup>7</sup> low-

energy photocuring,<sup>8</sup> and three-dimensional microfabrication.<sup>9,10</sup>

One of the most well-studied chromophores of this new generation is (*N,N*-diphenyl-7-[2-(4-pyridinyl)ethenyl]-9,9-didecylfluoren-2-amine), abbreviated AF50.<sup>11–13</sup> AF50 typifies a class of asymmetric donor–acceptor heterocyclic chromophores consisting of  $\pi$ -electron-donating and  $\pi$ -electron-accepting heterocyclic moieties separated by a conjugated aromatic core. When measured with nanosecond (ns) laser pulses, AF50 displays an effective two-photon cross-section value of up to  $19\,400 \times 10^{-50} \text{ cm}^4 \text{ s photon}^{-1}$ .<sup>14</sup> This is over 20 times greater than previous measured organic molecules such

\* Correspondence: jeff.baur@afrl.af.mil, richard.vaia@afrl.af.mil  
Deceased.

(1) Göppert-Mayer, M. *Ann. Phys., Lpz.* **1931**, *9*, 273.

(2) Peticolas, W. L. *Ann. Rev. Phys. Chem.* **1967**, *18*, 233.

(3) He, G. S.; Xu, G. C.; Prasad, Reinhardt, B. A.; Bhatt, J. C.; McKellar, R.; Dillard, A. G. *Opt. Lett.* **1995**, *20*, 435–437.

(4) Albota, M.; Brédas, J.-L.; Marder, S. R.; Perry, J. W.; Webb, W. W.; et al. *Science* **1998**, *281*, 1653–1656.

(5) Ehrlich, J. E.; Wu, X. L.; Lee, I.-Y. S.; Hu, Z.-Y.; Röckel, H.; Marder, S. R.; Perry, J. W. *Opt. Lett.* **1997**, *22* (24), 1843–1845.

(6) Bhawalker, J. D.; He, G. S.; Prasad, P. N. *Rep. Prog. Phys.* **1996**, *59*, 1041–1070.

(7) Parthenopoulos, D. A.; Rentzepis, P. M. *Science* **1990**, *248*, 73–76.

(8) Denny, L. R. Private communication

(9) Maruo, S.; Nakamura, O.; Kawata, S. *Opt. Lett.* **1991**, *16*, 1780–1782.

(10) Sun, H.-B.; Matsuo, S.; Misawa, H. *Appl. Phys. Lett.* **1999**, *74* (6), 786–788.

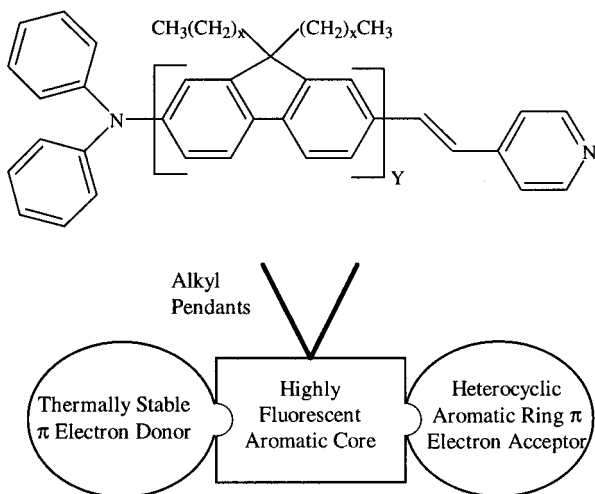
(11) He, G. S.; Yuan, L.; Cheng, N.; Bhawalker, J. D.; Prasad, P. N.; Brott, L. L.; Carlson, S. J.; Reinhardt, B. A. *J. Opt. Soc. Am. B.* **1997**, *14* (5), 1079.

(12) Fleitz, P. A.; Sutherland, R. A.; Strohkendl, F. P.; Larsen, J.; Dalton, L. R. Nonlinear Optical Liquids for Power Limiting and Imaging. *SPIE Proc.* **1998**, *3472*, 91–97.

(13) Reinhardt, B. A.; Brott, L. L.; Carlson, S. J.; Dillard, A. G.; Bhatt, J. C.; Kannan, R.; Yang, L.; He, G. S.; Prasad, P. N. *Chem. Mater.* **1998**, *10*, 1863–1874.

**Table 1. Structural Characteristics of Heterocyclic Chromophores**

| name  | no. of fluorenes ( $y$ ) | pendant length ( $x+1$ ) in carbons |
|-------|--------------------------|-------------------------------------|
| AF50  | 1                        | C10 (10 carbons)                    |
| AF100 | 1                        | C6                                  |
| AF60  | 1                        | C2                                  |
| AF210 | 2                        | C2, C2                              |

**Figure 1.** Molecular design of two-photon-absorbing vinyl pyridine-based heterocyclic chromophores.

as rhodamine B. The cross-section is considered "effective" because recent nonlinear transmission measurements using femtosecond (fs) pulses have suggested that the overall cross-section may consist of both a true two-photon absorbance and a single-photon excited-state absorbance.<sup>15</sup> The presence of this additional linear absorption process has hindered efforts to establish a comprehensive relationship between molecular structure and the molecule's two-photon absorption properties. Our current efforts focus on (1) elucidating the influence of local molecular environment on the excited states of asymmetric donor-acceptor chromophores and (2) determining the utility of one-photon spectroscopic techniques in establishing the structure-property relationships for their "effective" two-photon behavior.

Within this paper, we discuss the influence of local environment on the optical properties of AF50 and its structural analogues. These results have implications to two-photon applications that rely on up-converted fluorescence and give insight into potential contributions to the effective two-photon cross-section from excited-state absorbance. Using these results, guidelines can be developed for the synthesis of new chromophores with even larger effective two-photon cross-sections.

### Experimental Section

**Materials.** Table 1, in conjunction with Figure 1, summarizes the structural characteristics and the reference names of the chromophores examined in this study. The  $\pi$ -electron-accepting vinylpyridine and the  $\pi$ -electron-donating triarylamine are common to all the chromophores. The aromatic core consists of either one or two fluorene groups with pendant alkyl

chains varying from ethane (C<sub>2</sub>) to decane (C<sub>10</sub>). Details of the chromophore synthesis is discussed elsewhere.<sup>11</sup>

**Computation.** Semiempirical quantum chemical methods were used to determine the distribution of the frontier molecular orbitals in these molecules. Calculations were performed using HyperChem V5.01 for Windows. Structural optimization using AM1 (a modified neglect of diatomic overlap) was employed to find the minimum-energy configurations. Minimum-energy geometries were used for ZINDO/S CI calculations with the highest 15 occupied orbitals and the lowest 15 unoccupied (virtual) orbitals to determine the corresponding electronic spectrum (state dipole moment, transition dipole, and oscillator strength). The currently accepted values for the overlap weighting factors of 1.267 ( $\sigma-\sigma$ ) and 0.585 ( $\sigma-\pi$ ) were used.<sup>16</sup> Decreasing the  $\pi-\pi$  overlap weighting factor led to a red shift in S<sub>0</sub>-S<sub>1</sub> transition but did not significantly alter the correlations between the electronic spectrum and the molecular structure. The pendant alkyl chains on the fluorene were shown not to contribute electronically to the frontier orbitals and thus were replaced by a methane group to increase computational efficiency. The resulting methylated structures are henceforth referred to as AFX analogues.

**Characterization.** Photoluminescence and absorption measurements were conducted in various solvents including hexane, benzene, toluene, anisole, chlorobenzene, benzyl alcohol, tetrahydrofuran (THF), methylene chloride, ethanol, and hexane/THF mixtures of varying proportions. Spectroscopic and/or anhydrous grades of each solvent were used. Solutions were measured in UV-grade quartz cuvettes with path lengths ranging from 0.01 to 5 cm.<sup>17</sup> The linear absorption spectra were acquired using a Hewlett-Packard 8453A UV-visible spectrophotometer with 1-nm spectral resolution. The extinction coefficients were determined from the absorption measurement of at least 5 different solutions with concentrations typically ranging from 10<sup>-3</sup> M to 10<sup>-6</sup> M.

Linear photoluminescence measurements were made in a 2 mm path length cell using front face illumination. The 392-nm excitation radiation was obtained using a 300W Xe arc lamp tuned to a bandwidth of 4 nm using a 2400 line/mm grating. Fluorescence was collected between 400 and 700 nm using an EG&G 4000 optical multichannel analyzer with a spectral resolution of 0.5 nm and a 15-s signal integration. Nonlinear, or two-photon-excited, photoluminescence was measured using an argon ion pumped Ti:sapphire laser source producing a Gaussian pulse shape (90–200 fs width) at a repetition rate of 1 kHz with a peak power of approximately 1 GW/cm<sup>2</sup>. The fluorescence collection was taken at a right angle to the incident radiation using the EG&G 4000 optical multichannel analyzer. Photoluminescence quantum efficiencies were determined in both right angle and front-face configuration on the Spex Fluorolog III through comparison of luminescence intensity to three dyes of known quantum efficiency (rhodamine 6, coumarin 481, and coumarin 485) using standard methodology.<sup>18</sup>

### Results

To explore the influence of the local molecular environment on the series of dyes denoted in Figure 1 and their "effective" two-photon behavior, the influence of the local molecular environment on the excited state must be understood. Therefore, the dyes were both computationally modeled in the absence of a local molecular environment and spectroscopically characterized in a range of molecular environments.

(16) Del Bene, J.; Jaffe, H. H. *J. Phys. Chem.* **1968**, *48*, 1807.

(17) Degradation of AF50 solutions was occasionally observed after storage at room temperature and during the course of nonlinear fluorescence measurements. The nature of the chemistry underlying this degradation is currently being investigated but has been shown to not affect the discussed results.

(18) Demas, J. N.; Crosby, G. A. *J. Phys. Chem.* **1971**, *75*, 991–1024.

(14) He, G. S.; Yuan, L.; Cheng, N.; Bhawalker, J. D.; Prasad, P. N.; Brott, L. L.; Clarson, S. J.; Reinhardt, B. A. *J. Opt. Soc. Am. B* **1997**, *14* (5), 1079.

(15) Swiatkiewicz, J.; Prasad, P. N.; Reinhardt, B. A. *Opt. Commun.* **1998**, *157*, 135–138.

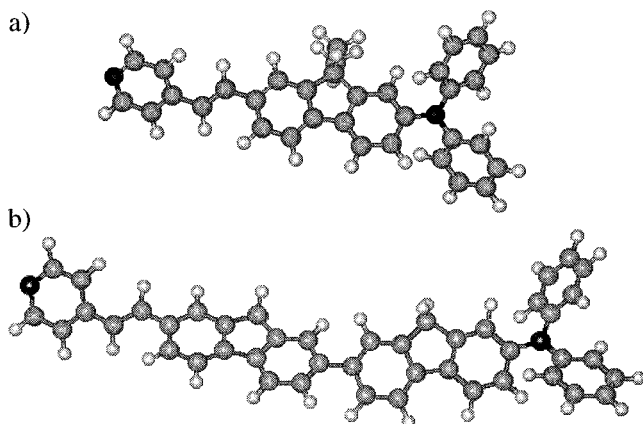


**Figure 2.** Equilibrium geometry for (a) AF50 and (b) AF210 analogues (methyl alkyl pendants).

**Computation.** In general, the visualization of ground-state geometry from which the molecule is excited is critical to interpret a molecule's spectroscopic characteristics. Figure 2 depicts the equilibrium geometry in a vacuum for AF50 and AF210 analogue determined from semiempirical AM1 calculations.

The AFX chromophores in Table 1 all share the same general equilibrium features. The molecules are highly extended (N–N separation: AF50 analogue  $\sim 14.9$  Å, AF210 analogue  $\sim 22.8$  Å), but are not completely planar. Steric interactions between the hydrogens that are ortho to the nitrogen in the triarylamine cause the aromatic groups of the donor to be oriented within planes that are each  $60^\circ$  removed from fluorene-amine plane and  $120^\circ$  removed from each other. Additionally, the five-member center ring of the fluorene introduces strain between the aryl groups and leads to the para units of the fluorene being  $15^\circ$  removed from collinear. For the bifluorene unit of the AF210 analogue, additional steric interactions between the fluorene moieties favor a nonzero torsion angle ( $41.5^\circ$ ,  $138.5^\circ$ ) between the groups. On the basis of heats of formation, the trans orientation of the vinyl pyridine acceptor is favored by  $\sim 3.3$  kcal/mol over the cis orientation. Finally, anti or syn configurations of the vinyl pyridine relative to the alkyl pendants of the fluorene are isoenergetic.

ZINDO/S CI calculations were performed on the ground-state geometry (trans orientation of the vinyl pyridine with an anti configuration) of the AFX analogues to gain insight into the nature of the excited states of the chromophores. Abridged results of the calculations for AFX analogues with a fluorene and bifluorene core are summarized in Table 2. The electron density distribution for the frontier orbitals (square of the molecular orbital wave functions) are shown in Figures 3 and 4.

For a single fluorene core (AF50 analog), the  $S_0$ – $S_1$  transition is primarily associated with a promotion of an electron from the HOMO to the LUMO. As shown in Figure 3, this transition leads to a large change in molecular dipole moment ( $\Delta\mu$ ) as the electron density is shifted from the triarylamine to the vinyl pyridine along the molecular axis. When such an extensive intramolecular charge transfer occurs in a local molecular environment of solvent molecules, the interaction and stabilization from those solvent molecules will lead

to fluorescence that is highly sensitive to the local molecular environment.

In contrast to the single fluorene core, the  $S_0$ – $S_1$  transition of the bifluorene analogue (AF210) has substantial contributions from HOMO – 1 and LUMO + 1 orbitals which results in a more diffuse distribution of electron density along the molecular axis for both the ground state and the excited state (Figure 4). Upon excitation, this results in only partial charge redistribution and a smaller  $\Delta\mu$  relative to the single fluorene analogue even though the distance between the triarylamine donor and vinyl pyridine acceptor is greater.

The increased influence of the bifluorene moieties in AF210 is also manifested in a substantial increase in the transition dipole, and thus the oscillator strength and extinction coefficient of the  $S_0$ – $S_1$  transition. Additionally, the finite torsion angle between the fluorene units disrupts extended conjugation in the ground state (HOMO – 1 and HOMO). Hence, instead of a substantial bathochromic shift of  $S_0$ – $S_1$ , the transition energy is comparable to that determined for a single fluorene core (AF50 analogue) and absorption is expected to occur in the same spectral region.

**Spectroscopy.** When the transitions discussed above occur within a solution rather than a vacuum, interactions with the local molecular environment (i.e., solvent–solute or solute–solute interactions) can influence the experimentally observed spectral properties. Initially, the optical behavior of AF50 is considered. For the concentration range ( $10^{-3}$  M to  $10^{-6}$  M) and solvents examined, the spectral shape of the absorption peaks and their calculated peak extinction coefficient remains relatively constant ( $\epsilon_{\lambda_{\max}} \approx 4.0 \times 10^4$  cm $^{-1}$  M $^{-1}$ ) with concentration. Figure 5 shows the relative influence of solvent polarity on the linear extinction coefficient. The strength of the transition (integrated area of a Gaussian curve fitted to the first transition) and corresponding oscillator strength varied by 12% for the examined solvents.

Overall, the experimental AF50 absorbance results indicate the absence of strong ground-state association (i.e., charge-transfer complex) and a good correlation with computational results. However, subtle changes such as peak broadening and red-shifting in different solvents indicate that interactions with the local molecular environment are present. For example, in hexane, AF50 displays a small amount of vibronic structure with the emergence of a shoulder near 400 nm and a peak maximum at 388 nm. The spectrum of the remaining solvents display a single peak (no vibronic structure) near 392 nm with the exception of benzyl alcohol which exhibits a maximum at 401 nm (a 15-nm red-shifted from hexane).

These minor shifts in the  $S_0$ – $S_1$  transition can be understood using mean-field interaction models such as that of Nicol.<sup>19</sup> In low dielectric solvents the dispersion properties of the solvent dictate the absorption behavior while in higher dielectric solvents the solvent–solute dipole–dipole interactions play a large role in decreasing the  $S_0 \rightarrow S_1$  transition energy. The broadening of the absorbance band with solvent polarity is also consistent with this trend. For example, the full width at half max (fwhm) of the fitted lowest energy absorbance band of AF50 in low dielectric ( $\epsilon < 9$ ) solvents

**Table 2. Energies (eV), Oscillator Strengths  $f$ , Dipole Moment  $\mu$ , and Components  $\mu_x$ ,  $\mu_y$ , and  $\mu_z$  (debye) and the Composition of the Excited States Wavefunctions Calculated by the ZINDO/S CI Method for the Lowest Energy, Spin-Conserved Transition**

| dye analogue | state            | energy | $f$   | $\mu$         | $(\mu_x, \mu_y, \mu_z)$                         | $S_0-S_1^a$  |
|--------------|------------------|--------|-------|---------------|---|--|
| AF50         | ground<br>$1^1A$ | 3.57   | 1.625 | 4.26<br>11.42 | (4.26, -0.022, -0.032)<br>(11.42, 0.003, 0.110) | 0.5525 (87,88)   |
| AF210        | ground<br>$1^1A$ | 3.58   | 2.723 | 4.13<br>8.48  | (3.89, 1.20, 0.678)<br>(7.98, 2.49, 1.42)       | 0.3591 (111,112);<br>-0.388 (110,112);<br>0.3712(111,113); |

<sup>a</sup> Transition from occupied to unoccupied molecular orbitals and associated coefficients

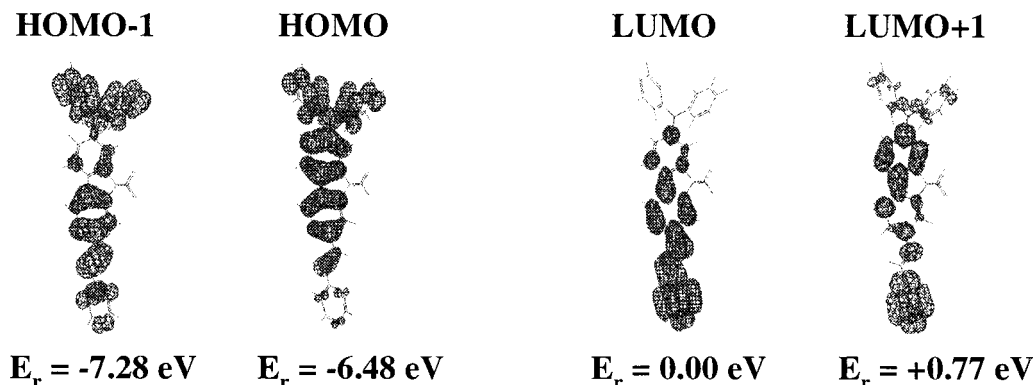


**Figure 3.** Square of the frontier molecular orbitals for AF50 analogue calculated using AM1 geometry and ZINDO/S CI method.  $\Delta E_r$  is the orbital energy relative to the LUMO. Orbital numbers are 86–89 (HOMO – 1 to LUMO + 1).

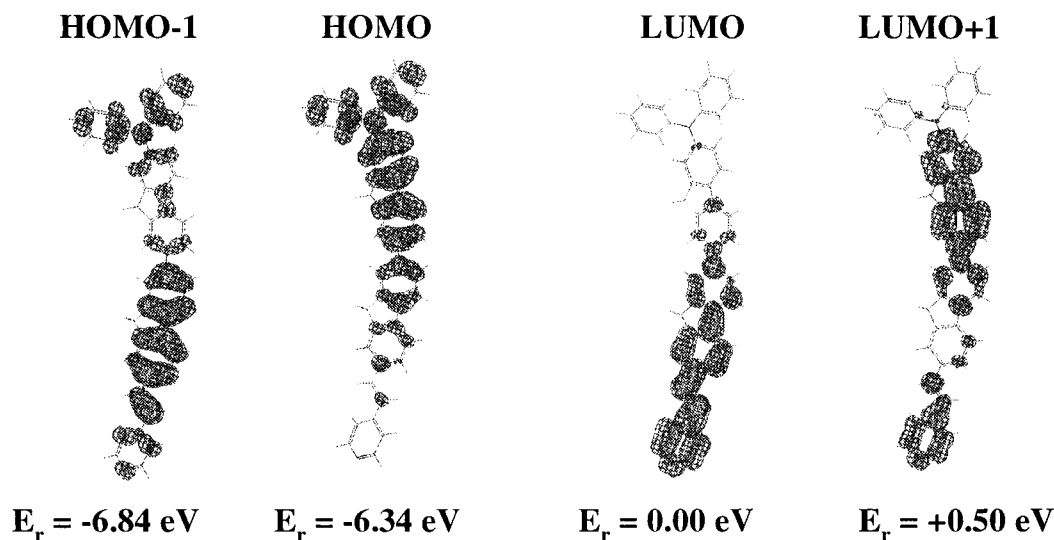


**Figure 4.** Square of the frontier molecular orbitals for AF210 analogue calculated using AM1 geometry and ZINDO/S CI method.  $\Delta E_r$  is the orbital energy relative to the LUMO. Orbital numbers are 110–113 (HOMO – 1 to LUMO + 1).

scale with the index of refraction, while the higher dielectric solutions ( $\epsilon > 9$ ) are even broader due to their dipole–dipole interactions. The large absorbance red-shift observed for AF50 in benzyl alcohol is likely linked to have both a high index of refraction (1.54 vs 1.34 for ethanol) and a high dielectric constant ( $\epsilon = 13.1$ ). Additionally, hydrogen bonding has been previously observed between pyridine and hydroxyl-containing molecules and may be occurring within protic solvents.<sup>20</sup>

The effect of the solvent environment on the linear photoluminescence of AF50 is shown in Figure 6. In contrast to the linear absorbance, the solvent polarity has a drastic effect on the spectral shape and wavelength of the luminescence. For nonpolar environments such as hexane, photoluminescence exhibits well-defined vibronic features with a maximum near 426 nm. For polar environments, only a single broad peak that

can be red-shifted by as much as 120 nm (ethanol) is observed. Overall, the fluorescence efficiency of AF50 in aprotic solvents remains constant ( $\sim 80\%$ ), but is quenched by as much as a factor of 4 in protic solvents such as benzyl alcohol and ethanol. This indicates that AF50 is a highly efficient chromophore with few intramolecular nonradiative decay paths. Nonradiative decay becomes prevalent only when specific intermolecular interactions such as those encountered in protic environments are present.

The absence of specific interactions between AF50 and aprotic solvents is demonstrated in Figure 7 where the photoluminescence for a series of hexane/THF mixed solvents with the same concentration of AF50 ( $6.8 \times 10^{-5}$  M) is shown. A continuous decrease in the vibronic structure and bathochromic shift occurs with increasing concentration of THF. The uniformity of the transfor-

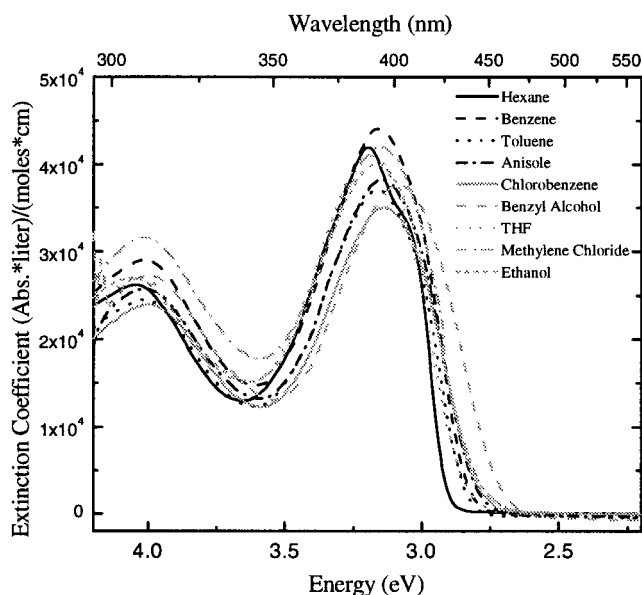


**Figure 5.** Extinction coefficients for AF50 in various solvents.

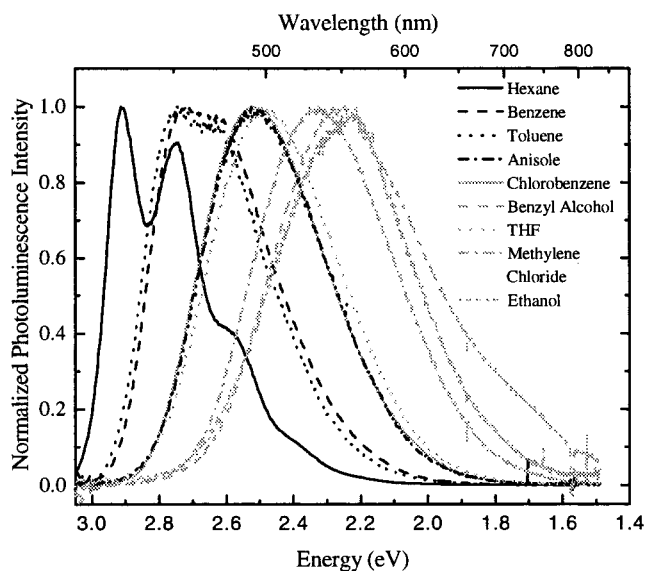


**Figure 6.** Linear photoluminescence of AF50 in various solvents. Note: All the data are normalized to a maximum luminescence intensity of 1.

mation as well as the constant fluorescence efficiency with changes in the solvent mixture indicates that the local molecular environment surrounding AF50 consists of a uniform mixture of hexane and THF molecules. Preferential segregation of one solvent resulting from specific solvent-chromophore interactions would cause a nonlinear or discontinuous shift in peak position and shape.

In addition to the spectral position of the fluorescence, the lifetime of the radiative decay from the excited state is altered by the average dielectric properties of the surrounding medium. This is expressed in the Strickler-Berg relation where the ratio of radiative lifetimes is proportional to the refractive index,  $n$ , and the maximum frequency of the luminescence,  $\nu_{em}$ .<sup>21</sup> Life-

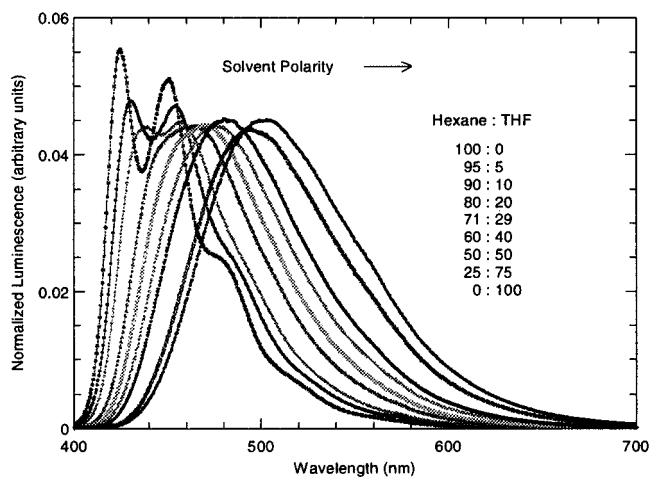


**Figure 7.** Linear photoluminescence of  $6.8 \times 10^{-5}$  M AF50 solutions with hexane/THF mixtures of varying proportions.

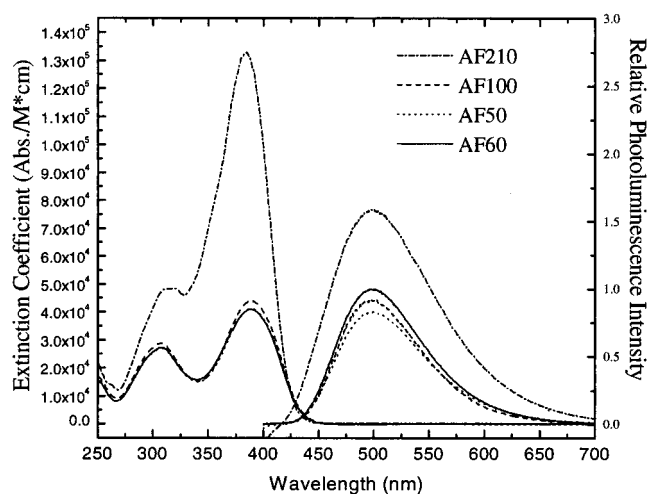


**Figure 8.** Extinction coefficient and relative photoluminescence intensity in THF for chromophores with 1 and 2 core fluorene moieties (AF60 and AF210, respectively) and for chromophores with increasing pendant length (AF60, AF100, and AF50).

times determined for AF50 in THF and hexane agree well with this relation ( $(\tau_1/\tau_2)^{-1} = 1.62$ ;  $(n_1^2\nu_{em,1}^3)/(n_2^2\nu_{em,2}^3) = 1.65$  where 1 = THF, 2 = hexane).

By comparing the observations made for AF50 with those from the rest of the series of dyes, the influence of variations in chemical structure on spectroscopic properties can be considered. Figure 8 compares the linear absorption and photoluminescence spectrum of AF50 (decane pendants, one fluorene) to AF60 (ethane pendants, one fluorene), AF100 (hexane pendants, one fluorene) and AF210 (ethane pendants, two fluorenes) in THF.

As suggested by computational results, the pendant length has little influence on the linear spectral properties of dyes with the same number of fluorene groups (AF50, AF60, and AF100). However, doubling the number of fluorene core groups, roughly triples the maximum in the extinction coefficient spectrum. Although the donor and acceptor end groups do red-shift the absorbance peak relative to unsubstituted or mono-

(19) Guilbault, G. G. *Practical Fluorescence*; Marcell Dekker: New York, 1990; p.135.

(20) Cesteros, L. C.; Isasi, J. R.; Katime, I. *Macromolecules* **1993**, *26*, 7256.

(21) Lackowicz, J. R. *Principles of Fluorescence Spectroscopy*; Plenum Press: New York, 1983.

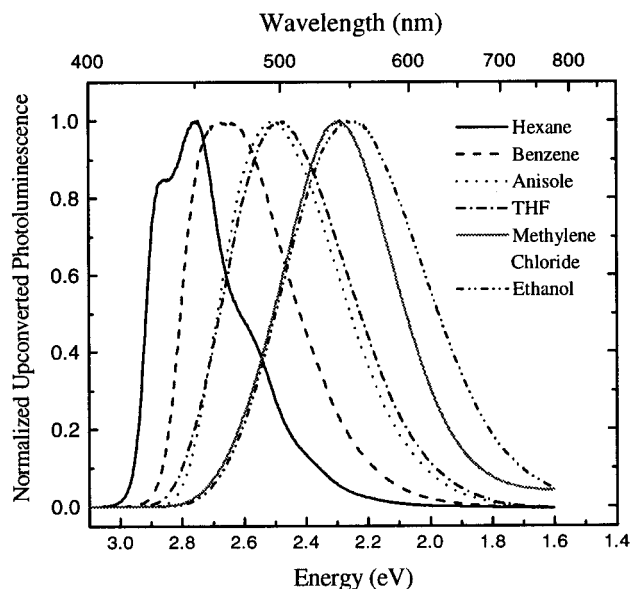


**Figure 9.** Shifting of upconverted photoluminescence of  $10^{-3}$  M AF50 solutions with solvents of increasing polarity.

substituted fluorene, this indicates that the fluorene core(s) are central to the linear absorbance. This is also shown computationally through their significant contributions to the frontier orbitals of the AF50 (Figure 3) and AF210 (Figure 4) analogues. Furthermore, the spectral positions of the absorbance peaks are also computationally predicted and experimentally found to be insensitive to the number of fluorene groups contained within the chromophore.

Similar to the spectral position of the absorbance peaks, the spectral positions of the photoluminescence peaks are also insensitive to the number of fluorene core groups. Due to an increase in absorbed energy from the previously mentioned tripling of the extinction coefficient, greater photoluminescence intensity is observed for a solution of AF210 than for a single-fluorene dye solution of the same concentration (Figure 8). However, the photoluminescence quantum efficiency, which is normalized for the amount of energy absorbed, actually decreases from 83% for AF50 to 53% for AF210 in THF.

When the up-converted, or two-photon-excited, photoluminescence of these dyes are measured, the spectral positions of the photoluminescence remains similar to the linear photoluminescence. Figure 9 illustrates the up-converted fluorescence of AF50 using  $\sim 160$  fs pulses for several solvents of varying polarity. Similar behavior has been reported for the up-converted fluorescence of AF50 when measured with 8-ns pulsed incident radiation.<sup>14</sup> The similarity between the one-photon- and two-photon-excited photoluminescence (femto- and nanosecond pulses) indicates that the luminescence is originating from the same solvent-sensitive excited state whether excited linearly, nonlinearly with femtosecond pulses, or nonlinearly with nanosecond pulses. For the applications that rely on a specific spectral position of the up-converted fluorescence such as two-photon photocuring, two-photon confocal microscopy, and photodynamic therapy, this environmental sensitivity will have significant implications.

## Discussion

By bringing computational and experimental results together into an existing spectroscopic model, the relative influence of the molecular environment on the spectral properties of these chromophores can be understood. Numerous theoretical models have extensively addressed the influence of the solvent on the linear photoluminescence. Some of these models incorporate both specific interactions, such as hydrogen bonding, and nonspecific interactions which can be described in terms of the index of refraction ( $n$ ) and the dielectric constant ( $\epsilon$ ) of the solvent.<sup>21</sup> One model that describes the nonspecific interactions between the solvent and a chromophore and that has been shown to be applicable for a wide range of compounds is given by the Lippert equation:<sup>22</sup>

$$\nu_{\text{abs}} - \nu_{\text{em}} = \frac{1}{2\pi\epsilon_0 hc} \frac{|\Delta\mu|^2}{a^3} \Delta f \quad (1)$$

where

$$\Delta f = \left[ \frac{\epsilon - 1}{2\epsilon + 1} - \frac{n^2 - 1}{2n^2 + 1} \right] \quad (2)$$

This model describes the chromophore as a dipole in a sphere of radius "a" within a dielectric medium ( $n$ ,  $\epsilon$ ) and predicts a linear correlation between Stoke's shift ( $\nu_{\text{abs}} - \nu_{\text{em}}$  in wavenumbers) and characteristics of the dielectric medium ( $\Delta f$ ). Upon excitation, the chromophore undergoes a change in dipole moment ( $\Delta\mu$ ) to which the solvent responds with a fast shifting of electron density, characterized primarily with  $n$ , and a slower dipolar rearrangement of the surrounding solvent molecules, characterized primarily with  $\epsilon$ . The energy of the resultant relaxed state is then dependent on the orientation polarizability ( $\Delta f$ , or "polarity", of the solvent with the more polar solvents being better able to stabilize the excited molecule and lower the emission energy. Therefore, upon emission, the luminescence from the polar solutions is red-shifted and gives larger Stoke's shifts than those of the nonpolar solvents. Chromophores exhibiting a large change in dipole moment upon excitation, like the AFX molecules, are expected to display very large Stoke's shifts in polar environments. Chromophores with smaller changes in dipole moment due to either symmetry or less charge transfer (i.e., weaker donor and/or acceptor moieties) are expected to have small, solvent-insensitive Stoke's shifts.

The linear correlation between Stoke's shifts and  $\Delta f$  predicted by the Lippert equation reasonably describes the influence of the solvent polarity on the fluorescence of AF50 (Figure 10). The Bakhshiev model with more sophisticated descriptions of solvent-solute interactions was also examined, but failed to give a significant improvement in the correlation between theoretical and experimental results ( $\sim 5\%$  increase in correlation constant  $R^2$ ).<sup>23</sup> The spectral data from the hexane/THF mixed-solvent solutions were incorporated into the Lippert framework using a "rule of mixtures" approach to determining the values of  $\epsilon$  and  $n$  for the mixed solution from the values of the substituent solvents (THF and hexane) and the relative proportion of each

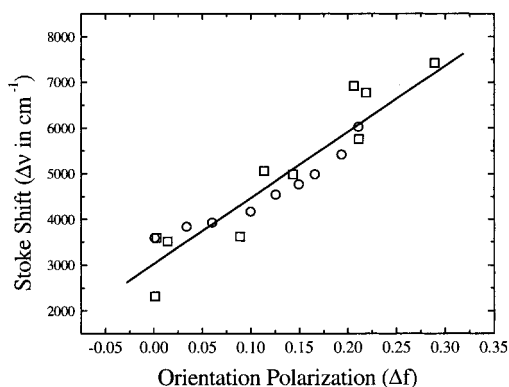


**Figure 10.** Linear fit of Stoke's shift versus orientation polarizability for AF50 in a variety of solvents to illustrate adherence of experimental data to Lippert equation. Open circles (○) represent data from THF/hexane solvent mixtures.

solvent. The agreement of the experimentally observed and the theoretically predicted behavior suggests that as assumed for the Lippert equation, the composition of the solvent cage surrounding the chromophore is roughly the same as the bulk composition and no significant solvent segregation occurs in the solvent cage. As previously discussed, the consistent luminescence efficiency of the hexane/THF solvent mixtures suggests that the chromophores within the two solvent environments have similar nonradiative mechanisms.

The linear absorption and photoluminescence of AF50 provides a basis from which the correlation between optical properties and molecular structure of the heterocyclic donor–acceptor chromophores can be understood. For example, computational results (Table 2) indicate that despite the 60% increase in the long axis of the molecule with the addition of the second fluorene to the AF50 structure, the change in molecular dipole upon excitation ( $\Delta\mu$ ) for AF210 is predicted to decrease. From the Lippert relation (eq 1), this should decrease the ratio of the square of the change in dipole moment over the volume of the solvent cage ( $|\Delta\mu|^2/a^3$ ) from both the decrease in  $\Delta\mu$  and the presumed increase in the molecular solvent cage volume and lead to smaller Stoke's shifts. The corresponding experimental Stoke's shifts for the one fluorene molecules (AF50, AF60, and AF100) and the two fluorene molecule (AF210) as a function of solvent polarity ( $\Delta f$ , eq 2) are shown in Figure 11. In contrast to this simple argument, both types of chromophores respond similarly to changes in the polarity of their environment.

Within the Lippert model, this can be understood to mean that either the  $\Delta\mu$  inferred from experiment data is larger than the calculated value or that the volume of the solvent cage ( $a^3$ ) is smaller than described by the length of AF210. For AF210 to have a larger  $\Delta\mu$  than AF50 in solution, either the electronic or molecular structure must be significantly altered relative to the vacuum calculations.

One plausible explanation is the presence of a twisted intramolecular charge transfer (TICT) state(s) in AF210, which changes the degree of conjugation between donor and acceptor moieties through a solvent sensitive molecular rotation.<sup>24</sup> However, the similarity in polarity

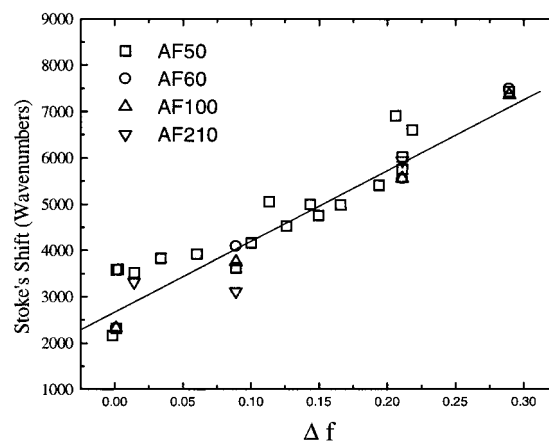


**Figure 11.** Stoke's shift vs solvent polarity for the examined heterocyclic dyes.

response of the absorbance and fluorescence energy of the AF210 and AF50 imply that the twisting between the two fluorenes of AF210 result in a species energetically similar to AF50. Typically, a molecule with a TICT state will have a fluorescence polarity response that is distinctly different in spectral position and lifetime from that given by the Lippert equation or the Stricker–Berg relationship, respectively.<sup>24</sup> However, as previously mentioned, the polarity response of AF210 follows the linear variation implied within the Lippert equation and the AF50, to which the AF210 responds almost identically, is in good agreement with the Stricker–Berg relation. Thus, the AF50 and AF210 are not believed to have a TICT state.

Another possibility is that the solvent cavity is smaller than predicted by the molecular dimensions of AF210. Although the commonly employed spherical solvent cavity approximation becomes poorer for more highly extended chromophores, consideration of more appropriate cavity shapes based on molecular dimensions (i.e., ellipsoidal cavities) cannot account for a decrease in cavity volume for AF210 relative to the AF50 analogues. Alternatively consider that as molecular size increases, orbital delocalization may occur on only a portion of the molecule. Thus, the effective solvent cage may be smaller than is suggested by the length of the molecule.

This is in agreement with the previously noted computational results that indicate the ground- and excited-state dipoles of the AF50 analogues are given primarily by the asymmetric charge distribution of the HOMO and LUMO and involves the entire molecule. In comparison, the ground- and excited-state dipoles of the AF210 analogues also involves the HOMO – 1 and LUMO + 1 states which lead to localized charge separation and a smaller effective solvent cage.

In addition to the core structure of the molecules, the effect of changing the length of the alkyl pendant was examined. From a molecular orbital perspective, the length of the pendant should not affect the  $S_0$ – $S_1$  transition because the atomic orbitals associated with the alkyl groups do not contribute to the frontier molecular orbitals of the molecule. As seen in and Figure 8, the extinction coefficient and absorption spectrum are

(22) Lippert, Von E. Z. *Electrochem.* **1957**, *61*, 962–975.

(23) Bakhshiev, N. G. *Opt. Spectrosc.* **1961**, *10*, 379.

(24) Maus, M.; Rettig, W.; Lapouyade, R. *J. Am. Chem. Soc.* **1999**, *103*, 3388.

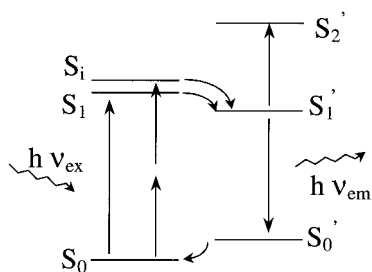


**Figure 12.** Hypothesized electronic states of AFX chromophores

nearly synonymous for AF50 (decane pendant), AF100 (hexane pendant), and AF60 (ethane pendant) when examined under identical conditions. It was considered that the luminescence might be influenced by the pendant length through the creation of a local cage around the excited molecular core that would buffer interactions with the solvent environment. However, the observed independence of the fluorescence yield and solvent-dependent Stokes shift to the pendant lengths examined (Figures 8 and 11) indicate that pendants longer than decane are necessary to observe this self-buffering phenomenon.

To understand the implications of the previously discussed linear structure–property relationships on the nonlinear absorption process, it is necessary to review the sensitivity of the “effective” two-photon absorption cross-section to changes in molecular structure and local molecular environment. Contrary to the linear absorption behavior, the effective nanosecond multiphoton absorption process has been shown to depend markedly on the solvent used. AF50, AF60, and AF100 have all been reported to display a 2–4-fold decrease in nanosecond cross-sectional values with increasing solvent polarity.<sup>11,25</sup> Additionally, their cross-sections were shown to decrease by as much as 20% when the pendant length was decreased from decane to ethane in a common solvent. This illustrates that the effective nonlinear process determined in these ns measurements are much more sensitive to changes in their local environment than the corresponding linear process.

One hypothesis, which is consistent with the linear absorbance and photoluminescence results and explains this sensitivity, is that a large contribution to the effective two-photon cross-section is associated with excited-state absorption from a solvent-sensitive excited state to an even higher energy excited state. As illustrated in Figure 12, the initially excited molecule relaxes to a lower energy state ( $S_1'$ ) following the instantaneous absorption of either one or two photons ( $S_0 \rightarrow S_1$ ). The excited-state absorption following the two-photon absorption of AF50 in THF has been reported to follow a complicated path with three distinctive relaxation lifetimes (6.6 ps, 0.11 ns, and 1.6 ns).<sup>15,16</sup> The longest lifetime is in agreement with the one-photon excited lifetime measured for AF50 in THF (2.2 ns), further indicating that the  $S_1'$  state plays a critical role in the nonlinear optical response of these molecules.

Since the correlation described by the Lippert equation is applicable to these molecules, it is proposed that

contribution to the “effective” two-photon absorption cross-section from the  $S_1' \rightarrow S_2'$  excited-state absorption can be understood using one-photon spectroscopic data that describes the solvent-dependent behavior of the  $S_1'$  state. The ability of the local molecular environment to alter the excited-state cross-section by either changing the strength or position of the  $S_1' \rightarrow S_2'$  transition energy will dictate the excited-state absorption efficiency and, thus, the effective two-photon cross-section. Since the lifetime of  $S_1'$  is approximately a nanosecond, shorter duration excitation pulses will produce smaller excited-state populations. Thus, the probability of excited-state absorption is decreased and the measured cross-section is correspondingly decreased. This trend is consistent with the increase in effective two-photon cross-section by several orders of magnitude in going from the 160-fs pulses to 8-ns pulses.<sup>13</sup> Additionally, two-photon cross-sections measurements made with femtosecond pulses (160–433 fs) by several different researchers in acetone, hexane, benzene, THF, and ethanol also indicate less sensitivity to the local molecular environment.<sup>12,15,26</sup>

### Conclusions

In conclusion, the relationship between the chemical structure, the local solvent environment, and the resultant optical properties were examined for a series of asymmetric heterocyclic chromophores. It was found that (1) the stabilization of the linearly induced long-lived excited state by the local molecular environment can be predictably described with the Lippert equation, that (2) this understanding is applicable to the two-photon absorbing dyes and their excited-state absorption, and that (3) one-photon spectroscopic techniques offer a simple way to help establish structure–property relationships for “effective” two-photon behavior.

It is suggested that the measured effective two-photon absorption cross-section is characterized by a true two-photon absorption and a subsequent excited-state absorption. In addition to pulse width, the excited-state absorption is highly sensitive to the local molecular environment—a molecular environment that can be accurately described by the Lippert equation. Thus, it should be possible to improve the apparent nanosecond nonlinear cross-section via optimization of the excited-state absorption by controlling the local environment of the chromophore either synthetically or through the proper processing of the chromophores.

**Acknowledgment.** The authors dedicate this paper to the memory of Bruce A. Reinhardt who passed away during the preparation of this manuscript. His technical leadership and jovial disposition will be greatly missed. This work was supported by the Polymer Branch of the U.S. Air Force Research Laboratory and the U.S. Air Force Office of Scientific Research through contract F4962093C0017. The authors acknowledge individuals at the SPEX Industries for their assistance in making photoluminescence lifetime measurements and to DeLyle Eastwood of the Air Force Institute of Technology for assistance in making photoluminescence quantum efficiency measurements.

CM990258S

(25) Baur, J. W.; Alexander, M. D.; Banach, M.; Reinhardt, B.; Prasad, P. N.; Yaun, L.; Vaia, R. A. In *Nonlinear Optical Liquids for Power Limiting and Imaging*. SPIE 1998, 3472, 70–79.

(26) Kirkpatrick, S.; Alexander, M. Jr.; Pooler, E. S.; Baur, J. W. Manuscript in preparation.